Analysis of Fe(Se,Te) Films Deposited on Unbuffered Invar 36

G. Sylva, A. Malagoli, E. Bellingeri, M. Putti, C. Ferdeghini, A. Vannozzi, G. Celentano, S. C. Hopkins, A. J. G. Lunt, A. Ballarino, and V. Braccini

***Abstract* — In this paper, the feasibility of producing Fe(Se,Te) coated conductors on cost-effective, unbuffered Invar 36 substrates is studied. A suitable substrate with a sharp {001}<100> texture and a misorientation angle lower than 10° was developed, and the possibility of growing epitaxial thin films without any buffer layer was demonstrated. It was also shown that the presence of a Fe(Se,Te) seed layer can improve the in- and out-of-plane orientation of the film. A high resolution scanning electron microscopy study was performed, and the absence of a superconducting transition has been attributed to Ni poisoning based on X-ray microanalysis.**

***Index Terms*— Iron Based Superconductors, Fe(Se,Te) thin films, Coated Conductors, Invar 36 alloy, Biaxial Texturing, Pulsed laser Deposition**

I. Introduction

THE iron chalcogenides, also called the 11 family ($FeSe_xTe_{1-x}$), are the simplest Iron Based Superconductors (IBS), and they are quite attractive because of their comparative ease of fabrication and the absence of toxic arsenic. The 11 family shows an upper critical field, B_{c2}, of about 50 T, and the critical temperature T_c can be enhanced from the 15 K of the bulk samples up to 21 K in thin films thanks to substrate-induced compressive strain [1]. Due to their high B_{c2}, potentially high critical current density (J_c) and low anisotropy the iron chalocogenides are particularly promising for applications.

In IBS, as in the cuprate high temperature superconductors (HTS), the J_c depends on the misorientation angle of grain boundaries (θ_{GB}) [2]. For this reason, the Coated Conductor (CC) technology established for HTS, which provides a biaxial alignment of grains, is a promising route for improving the performance of IBS. Fortunately, the critical misorientation angle at which J_c starts to decrease exponentially is around 9° for 11 phase, much larger than the ~3° reported for $YBa_2Cu_3O_{7-x}$ (YBCO) [3][4]. This is a great advantage for the fabrication of CCs since requirements on the in-plane alignment of buffer layers are less demanding. 11 thin films have been successfully grown on single crystalline substrates and on technical textured metallic templates. $FeSe_{0.5}Te_{0.5}$ thin films grown on Hastelloy substrates, with biaxially aligned MgO layers made by Ion-Beam Assisted Deposition (IBAD), have been reported with a J_c above 0.1 MA/cm^2 at 4.2 K and in magnetic fields up to 25 T [5]. It was also demonstrated that a CeO_2 buffer can significantly improve the J_c of 11 films deposited using Rolling-Assisted Biaxially Textured Substrates (RABiTS) [6]. Recently, a J_c of 0.43 MA/cm^2 at 4.2 K in self-field was obtained in a 11 film deposited by Pulsed Laser Deposition (PLD) on a less well textured metal template with a biaxially aligned IBAD $LaMnO_3$ buffer layer [7]. In IBS CCs, the processing temperature can be much lower (below 400 °C) than for YBCO (800 °C), and oxygen annealing is not required. Therefore, thinner and less complicated structures are expected to be suitable: $FeSe_{0.1}Te_{0.9}$ thin films with a T_c of 10 K, and a J_c of 2.1 × 10^4 A/cm^2 in self-field, were thus obtained on a metallic substrate with only one Al_2O_3 amorphous buffer layer [8]. The development of simpler substrates made of a commercial low cost alloy could be a new route for the production of cost-effective 11 CCs. Invar 36 (nominal composition Ni 36 wt%, Mn + Si + C <1 wt%, the balance Fe), which has a suitable lattice parameter for 11 thin film deposition, was selected for investigation.

In the present work, a biaxially textured Invar 36 substrate was prepared, epitaxial thin films of the 11 phase were deposited on that substrate without any buffer layer, and a detailed analysis of the texture was performed. Finally, an attempt was made to measure a superconducting transition resistively, and the cross-section of the CC was analysed by scanning electron microscopy (SEM).

II. Experimental Details

A. Texturing of the substrate

Invar 36 is a commercial Ni/Fe alloy, well known for its very low thermal expansion coefficient. It has a face centered cubic

Manuscript receipt and acceptance dates will be inserted here. This work is supported by CERN within a collaborative project defined by Addendum FCC-GOV-CC-0086 to the Memorandum of Understanding for the Future Circular Collider Study (FCC Study) *(Corresponding author: Valeria Braccini.)*

G. Sylva and M. Putti are with Physics Department, University of Genova, 16146 Italy and also with CNR-SPIN, C.so F. M. Perrone, 24, 16152 Genova, Italy (e-mail: giulia.sylva@spin.cnr.it; putti@fisica.unige.it).

A. Malagoli, E. Bellingeri, C. Ferdeghini and V. Braccini are with CNR-SPIN, C.so F. M. Perrone, 24, 16152 Genova, Italy (e-mail: andrea.malagoli@spin.cnr.it; emilio.bellingeri@spin.cnr.it; carlo.ferdeghini@spin.cnr.it valeria.bracini@spin.cnr.it).

A. Vannozzi and G. Celentano are with ENEA Frascati Research Centre, Frascati 00044, Italy (e-mail: angelo.vannozzi@enea.it; giuseppe.celentano@enea.it)

S. C. Hopkins, A. J. G. Lunt and A. Ballarino are with the European Organization for Nuclear Research (CERN), CH-1211 Geneva 23, Switzerland (e-mail: simon.hopkins@cern.ch; alexander.lunt@cern.ch; amalia.ballarino@cern.ch).

structure, space group Fm-3m, with a lattice parameter of about 0.359 nm. This is very close to the in-plane lattice parameter of tetragonal 11 (0.379 nm), so an epitaxial relation (001)[100] 11 ‖ (001)[100] Invar 36 can be expected. Moreover, since both the Invar 36 alloy and 11 phase are mainly composed of Fe, chemical compatibility seems to be possible. Glowacki *et al.* have demonstrated the possibility of obtaining a biaxially textured Invar tape that can be suitable as a substrate for YBCO CCs [9].

Starting from a commercially available Invar 36 rod, a suitable process to obtain cube texturing with a combination of cold drawing, cold rolling and recrystallization heat treatment was developed. Starting from a 10 mm rod, drawing (10% cross section reduction) followed by flat rolling was applied (10% thickness reduction steps at a line speed v of 0.7 – 2 m/s). With this procedure, tapes with a thickness of 50 – 120 µm were obtained, with a maximum thickness reduction of 99.5%.

After deformation, all tapes were subjected to a recrystallization heat treatment, which was performed in a Lenton furnace (LTF 16/50/180) at 1000 °C for 1 to 2 hours. Due to the high sensitivity of Ni/Fe alloys to oxidation, before heat treatment the tube was evacuated, and the heat treatment was performed in flowing Ar/H_2.

All the tapes were characterized by X-ray diffraction (XRD) before and after heat treatment with a four-circle diffractometer. Microstructural investigations were carried out by electron backscattering diffraction (EBSD) using an Oxford Nordlys Nano EBSD system installed on a Leo 1525 field-emission scanning electron microscope (SEM). Kikuchi patterns were acquired and indexed using the Ni m3m cubic phase with an Oxford AZtec software. For EBSD maps, the region of interest was sampled using a square grid with a pixel size of 6.25 µm^2, and tilt correction was applied. EBSD misorientation maps and pole figures were generated using HKL Channel 5 software, performing noise reduction by extrapolating both zero solutions and wild spikes.

B. *11 deposition*

11 thin films were deposited on Invar 36 substrates in an ultra-high vacuum PLD system equipped with a Nd:YAG laser at 1024 nm, using a $FeSe_{0.5}Te_{0.5}$ target directly synthesized with a two-step method [10]. The optimized laser parameters to obtain high quality epitaxial 11 thin films were a 3 Hz repetition rate, a 2 J/cm^2 laser fluency (2 mm^2 spot size) and a 5 cm distance between target and sample [11]. The deposition was carried out at a residual gas pressure of 10^{-8} mbar while the substrate was kept at a temperature between 200 °C and 300 °C. Since the thermal expansion coefficient of the Invar 36 alloy starts to increase very rapidly above 200 °C [12], the deposition temperature was maintained as low as possible to avoid the fracture of the film, although too low a temperature may have a negative effect on the texture of the film. For this reason, a 11 seed layer about 200 nm in thickness was introduced, following Molatta *et al.* [13], who demonstrated that it is possible to increase the epitaxy of 11 thin films on MgO substrates using this approach. This allows a better matching between superconducting film and substrate, increasing the in-plane and out-of-plane orientation. The seed layer was deposited at 400 °C and 10 Hz: under such conditions the phase does not grow to be superconducting, even on single crystal substrates. After the deposition of the seed layer, the substrate was cooled down to 200 °C while the deposition continued at 3 Hz.

To characterize the 11 film and substrate interface in cross-section, a lamella was prepared by Focused Ion Beam (FIB) milling and analyzed by SEM, using a Zeiss XB540 FIB/SEM. A 1 × 1 cm^2 section of the sample was prepared and mounted on an SEM stub using silver paint. A Pt protection barrier was deposited, first with electron beam induced deposition and then by ion beam induced deposition. A 15 × 17 × 0.1 µm^3 lamella was prepared in the cross-section of the film perpendicular to the rolling direction, of which a 5 × 5 × 0.1 µm^3 region was thinned for imaging. Scanning transmission electron microscopy (STEM) imaging was performed in high-resolution mode, with a probe current of 413 pA and an accelerating voltage of 30 kV. For compositional analysis, Transmission Energy Dispersive X-ray Spectroscopy (TEDS) was performed at an accelerating voltage of 30 kV and a current of 2 nA.

III. RESULTS AND DISCUSSION

A. *Texture analysis of Invar 36 Substrate*

The 70 µm thick Invar 36 tape showed the best results in terms of biaxial texturing. Fig. 1 shows the θ–2θ scan of the as-received Invar 36 rod (black), the 70 µm tape produced by mechanical deformation before (dark grey) and after (light grey) the heat treatment. The as-received rod shows three crystalline peaks characteristic of the alloy. After mechanical deformation the (220) and (200) peaks are present, while after the heat treatment the tape shows only the (200) reflection, meaning that a preferential orientation (001) was obtained.

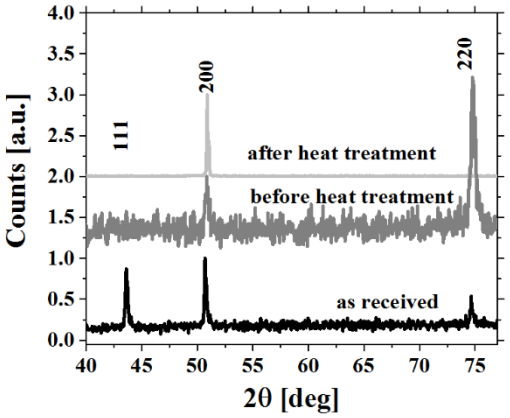

Fig. 1. θ–2θ analysis of Invar 36 starting from the as received rod (10 mm diameter) in black, to the final 70 µm tape before (dark grey) and after (light grey) heat treatment.

The ω scan, shown in Fig. 2a, highlights an out-of-plane orientation along the (200) direction with a full-width at half-maximum (FWHM) of 6° in the Rolling Direction (RD) and of 9° in the Transverse Direction (TD). Fig. 2b reports the ϕ scan along the (220) direction of the Invar tape, which shows an in-plane orientation with a FWHM of about 10°. The microstructure of

the Invar 36 substrate has been analyzed by means of EBSD analysis

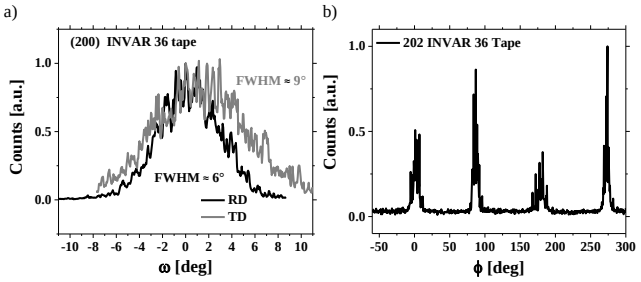

Fig. 2. a) ω scan of a 70 µm thick Invar 36 tape in the rolling direction (black curve) and the transverse direction (grey curve). b) ϕ scan along the (220) direction of a 70 µm thick Invar 36 tape.

Fig. 3 shows the EBSD map (a) and the corresponding pole figures (b), with points colored according to the local misorientation angle with respect to the ideal {001}<100> orientation, as shown in the legend of Fig. 3 (c). In addition, grain boundaries above 2° and 10° are shown in Fig. 3a (thin lines = above 2°, thick lines = above 10°). Kikuchi patterns were well indexed using the Ni Fm-3m cubic phase. The Invar 36 substrate shows a rather sharp {001}<100> texture, with 92.2% of points oriented within 12°. A minor contribution due to cubic twins is visible in the pole figures as scattered poles well indexed as {221}<122>. Although there is room for improvement, the microstructure of the Invar 36 substrate already looks suitable for the development of 11 based CCs. In fact, the microstructure of the Invar 36 substrate is well connected with a threshold angle of 7° (above which the microstructure becomes unconnected and no percolative path can be found [9]), which is below the critical misorientation angle for 11 (around 9°).

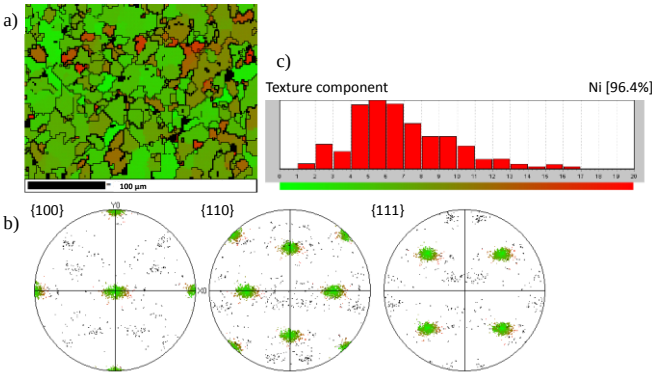

Fig. 3. (a) EBSD map and (b) pole figures of the Invar 36 substrate. Kikuchi patterns were indexed using the Ni m3m cubic phase. The rolling direction is aligned vertically. Points are displayed depending on their misorientation with respect to the ideal {001}<100> orientation. The legend (c) shows the distribution of the acquired points with 1° class width as a function of the misorientation angle from 0° (green) to 20° (red). Points unindexed or above 20° are black. GBs above 2° (thin line) and 10° (thick line) are included in the map.

B. *Texture analysis of 11 thin films*

After preparation of a suitable Invar 36 substrate, 11 thin films were deposited on the metallic tape without any buffer layer. The best results were obtained when depositing the film at 300 °C without seed layer or at 200 °C with a seed layer. In this section, a comparison between these two samples is presented. In Fig. 4a the θ–2θ scan of the 11 film grown at 300 °C (black) is compared with a film deposited at 200 °C on a seed layer (grey). Both samples show *c*-oriented growth. The epitaxy of the films was confirmed by ω scans along the (100) direction of the 11 phase performed in the rolling and transverse directions (Fig. 4 c, d). Both films show an out-of-plane orientation comparable to that of the substrate, and the seed layer causes a significant improvement in the out-of-plane orientation of the film: the misalignment angle is reduced by about 1° in both directions (Fig. 4c, d). The presence of the seed layer also causes an improvement in the in-plane orientation of the film (Fig. 4b). Moreover, the film without a seed layer shows a double in-plane orientation, corresponding to two different growth directions of the film: (001)[100] and (001)[110]. Conversely, the seed layer provides a single in-plane orientation (001)[001], and a reduction in the FWHM of about 2°.

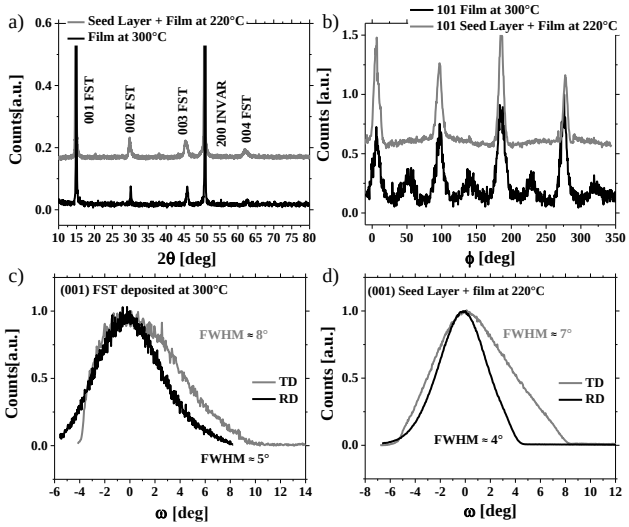

Fig. 4. a) θ–2θ scan of 11 thin film on Invar 36 substrate; b) ϕ scan of the (010) direction of 11 thin film on Invar 36; c) and d) ω scans along the (100) direction of the 11 thin film on Invar 36 measured along the RD and the TD of the tape.

C. *Coated Conductor Characterization*

Resistivity measurements performed on the films revealed that they are not superconducting, despite the good degree of alignment demonstrated by XRD. To investigate the causes, a cross-sectional lamella was prepared by FIB and analyzed by SEM. The STEM micrograph in Fig. 5 shows the cross-section of the sample. The 11 film have a total thickness of ~450 nm, and it appears that the seed layer and film can be resolved from each other, with an interface ~210 nm above the substrate. Some microstructural features are continuous across that interface, supporting the observation of epitaxial growth by XRD. A significant amount of porosity is evident, but largely concentrated at the interfaces, with larger voids at the substrate surface and smaller ones above the seed layer. TEDS mapping (Fig. 6) confirmed the expected distribution of key elements: C and Pt in the protective coating, Se and Te primarily in the films, Ni primarily in the invar substrate, and Fe in both the films and the substrate. O was detected throughout. For a more detailed analysis, a line scan was performed (Fig. 7). The overall distribution

is as described above, but it is interesting to note the small peak in oxygen concentration at the film surface and the substrate interface.

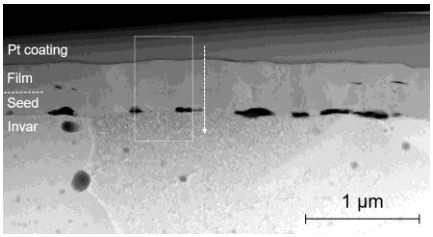

Fig. 5. An annotated STEM micrograph (outer high-angle annular dark-field imaging detector) of the coated conductor cross-section showing the substrate, Fe(Se,Te) films (total thickness ~450 nm) and protective layer. The overlays show the approximate location of the TEDS map (Fig. 6) and line scan (Fig. 7).

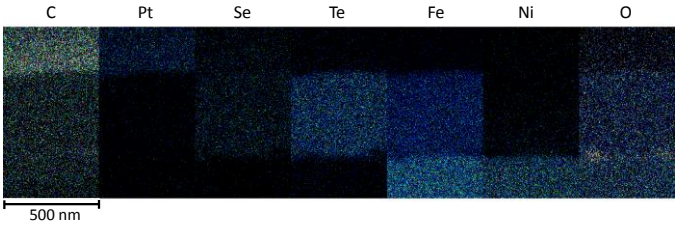

Fig. 6. A TEDS map showing the distribution of C (quantified from K series lines), Pt (L), Se (K), Te (L), Fe (K), Ni (K) and O (K). The region corresponds approximately to the dotted box in Fig. 5.

TEDS maps also tentatively suggest that the oxygen concentration peaks at the voids. It is therefore possible that defects are associated with localized surface oxidation. Interpretation of the absolute concentrations is hampered by the inclusion of C and Pt, which are largely artefacts of sample preparation. To clarify the composition of the film, the concentrations in this region were re-normalized to include only the elements present by design, Fe, Ni, Te and Se. The resulting line scan in Fig. 8a shows a sharp change of composition at the substrate interface, and a reasonably uniform concentration of Fe, Te and Se throughout the film. However, in the vicinity of the substrate, some Ni is present and the Fe concentration decreases. Averaging over a larger area, the average composition of the film and seed layer is 49.9 at% Fe, 22 at% Se, 25.6 at% Te and 2.5 at% Ni, close to the intended $FeSe_{0.5}Te_{0.5}$ composition.

To verify the compositional uniformity of the film, the data are re-plotted relative to the average film concentration in Fig. 8b, after smoothing. Ni clearly shows a diffusional profile through the film, with traces reaching the film surface, but with a change in gradient between the seed layer and the film. In contrast, the Fe concentration is very uniform across the film (note the different scale); within the seed layer, the Fe concentration (and perhaps also Te) decreases to balance the high Ni concentration. The apparent diffusion of Ni into seed layer and film is the most likely cause of the suppression of superconductivity. A similar phenomenon was also reported for a 11 wire produced by a Powder In Tube (PIT) method using a Ni sheath: in that case the iron of the 11 phase diffused into the Ni sheath, forming particles of a Fe–2 at% Ni solid solution and suppressing superconductivity [14]. It should be noted that local defects associated with voids and/or surface oxides may also contribute to this behavior, for example by locally disrupting the texture. Further investigation is needed to confirm this, but given the good macroscopic texture in the film (which grows epitaxially on the seed layer) and the larger defects at the substrate, it is believed this is a secondary effect.

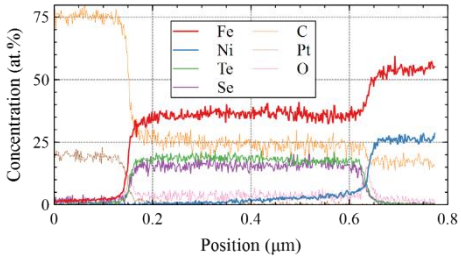

Fig. 7. A TEDS line scan showing the composition of all quantified elements as a function of position, from protective coating to substrate. The region corresponds approximately to the line in Fig. 5.

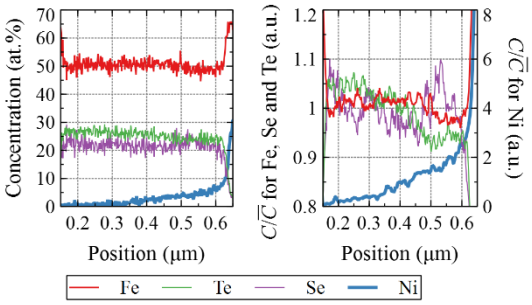

Fig. 8. Renormalization of the line scan composition data in Fig. 7 to include only the elements present in the Fe(Se,Te) film, which extends over a position range of approximately 0.16–0.61 μm.: (a) concentration *C*, without smoothing and (b) the concentration normalized by the average film composition, after moving average smoothing.

STEM analysis underlines the fundamental role of a buffer layer. Although the deposition temperature of the film is quite low compared to the temperature used for the heat treatment of 11 PIT wire [14] or YBCO deposition, and even if the 11 is deposited in ultra-high vacuum, Ni diffusion and partial oxidation of the substrate appear unavoidable, probably due to the local heating induced by the plasma.

IV. Conclusion

In this paper the feasibility of producing 11 CCs using a cost-effective Invar 36 substrate without any buffer layer was studied. The possibility of obtaining a metallic biaxially textured substrate with an in-plane and out-of-plane orientation suitable for the deposition of 11 thin films was demonstrated, and such films were successfully deposited. The in-plane and out-of-plane orientation of the film can be improved using a non-superconducting 11 seed layer, reaching a misorientation angle (both in plane and out of plane) lower than 9°, the critical angle at which J_c starts to decrease exponentially in 11 phase. Despite the good orientation of the films, they do not show a superconducting transition. STEM analysis performed on a cross-sectional lamella prepared by FIB revealed local oxidation of the substrate at the interface with the film and significant Ni diffusion from the substrate to the film. This Ni poisoning is most likely the cause of the suppression of superconductivity.

REFERENCES

[1] E. Bellingeri *et al.*, "Tuning of the superconducting properties of $FeSe_{0.5}Te_{0.5}$ thin films through the substrate effect", *Supercond. Sci. Technol.*, vol. 25, 2012, Art. no. 084022

[2] T. Katase *et al.*, "Advantageous grain boundaries in iron pnictide superconductors", *Nat. Commun*. vol. 2, 2011, Art. no. 409

[3] W. Si *et al.*, ''Grain boundary junctions of $FeSe_{0.5}Te_{0.5}$ thin films on $SrTiO_3$ bi-crystal substrates'' *Appl. Phys. Lett.*, vol. 106, no. 3, 2015, Art. no. 032602

[4] E. Sarnelli *et al.*, "Properties of Fe(Se, Te) Bicrystal Grain Boundary Junctions, SQUIDs, and Nanostrips", *IEEE Trans. Appl. Supercond.*, vol. 27, 2017 Art. no. 7400104

[5] W.D. Si *et al.*, "Iron-chalcogenide $FeSe_{0.5}Te_{0.5}$ coated superconducting tapes for high field applications'' *Appl. Phys. Lett.*, vol. 98, 2011, Art. no. 262509.

[6] W.D. Si *et al.*, "High current superconductivity in $FeSe_{0.5}Te_{0.5}$-coated conductors at 30 tesla", *Nat. Commun.*, vol. 4, 2013, Art. no. 1347.

[7] Z. Xu, Y. Pusheng, M. Yanwei and C. Chuanbing, "High-performance $FeSe_{0.5}Te_{0.5}$ thin films fabricated on less-well-textured flexible coated conductor templates", *Supercond. Sci. Technol.*, vol. 30, 2017, Art. no. 035003

[8] J. Huang *et al.*, "A simplified superconducting coated conductor design with Fe-based superconductors on glass and flexible metallic substrates", *J. Alloys Comp.* vol. 647, 2015, pp. 380-385

[9] B. A. Glowacki e*t al.*, "Texture development in long lengths of NiFe tapes for superconducting coated conductor", *J. Mater. Sci.*, vol. 37, 2002, pp. 157– 168

[10] A. Palenzona *et al.*, ''A new approach for improving global critical current density in Fe($Se_{0.5}Te_{0.5}$) polycrystalline materials", *Supercond. Sci. Technol.*, vol. 25, 2012, Art. no. 115018

[11] V. Braccini *et al.*, ''Highly effective and isotropic pinning in epitaxial Fe(Se,Te) thin films grown on CaF_2 substrates'' *Appl. Phys. Lett.*, Vol. 103, 2013, Art. no. 172601

[12] M.A. Hunter, ''*Low expansion alloy*'' Metal Handbook 8th ed. Vol.1, American Society for metals, Metals Park, Ohio 1971.

[13] S. Molatta, S. Haindl, S. Trommler, M. Schulze, S. Wurmehl and R. Hühne, ''Interface control by homoepitaxial growth in pulsed laser deposited iron chalcogenide thin films'' *Sci. Rep.* vol. 5, 2015, Art. no. 16334

[14] M. Palombo *et al.*, "Exploring the feasibility of Fe(Se,Te) conductors by ex-situ powder-in-tube method", *J. Appl. Phys.*, Vol. 117, 2015, Art. no. 213903